Journal of Catalysis **203,** 192–200 (2001)
doi:10.1006/jcat.2001.3297, available online at http://www.idealibrary.com on IDEAL®

A Kinetic Investigation of the Effects of Fluorine and Nickel on the HDN of Toluidine on Fully Sulfided Tungsten Sulfide Catalysts

Mingyong Sun and Roel Prins[1]

Laboratory for Technical Chemistry, Swiss Federal Institute of Technology (ETH), 8093 Zurich, Switzerland

Received April 9, 2001; accepted June 7, 2001; published online August 28, 2001

The effects of fluorine and nickel on the hydrodenitrogenation of *o*-toluidine on alumina-supported tungsten catalysts were studied in a continuous-flow reactor at 320 to 370°C and 3.0 MPa. The catalysts were prepared from ammonium tetrathiotungstate and were fully sulfided. The kinetic data were obtained by varying the initial partial pressure of the reactant and the reaction temperature; Langmuir–Hinshelwood models were used to fit the kinetic data. The simultaneous reactions of cyclohexene and *o*-toluidine enabled us to study the inhibition effect of *o*-toluidine on the hydrogenation of cyclohexene and to determine the difference between the sites for these reactions. The kinetic data suggest that the formation of toluene and 2-methylcyclohexylamine from *o*-toluidine occurs through a common partially hydrogenated intermediate, dihydrotoluidine, which leads to toluene by elimination and 2-methylcyclohexylamine after further hydrogenation. Fluorination changes neither the activation energies for the hydrogenation reaction nor the heat of adsorption of *o*-toluidine. Fluorine thus does not change the intrinsic properties of the active sites but does affect the apparent activity by influencing the number of active sites. Only a change in the morphology of the metal sulfide surface, by stacking, can explain the fluorine effect. Addition of nickel changes the nature of the active site by creating a nickel-associated sulfur vacancy, which is highly active for hydrogenation.

Key Words: **hydrodenitrogenation; fluoride effect; nickel; tungsten sulfide; kinetics; *o*-toluidine; cyclohexene.**

INTRODUCTION

Fluorination of alumina increases the activity of alumina-supported molybdenum (1–4) and tungsten (5, 6) catalysts for hydrodesulfurization (HDS) and hydrodenitrogenation (HDN). These higher activities have been ascribed to changes in the dispersion of the metal species in the oxidic precursor of the catalyst (3), to enhanced acidity (2, 5–7), and to increased sulfidability and to changes in the morphology of the WS_2 crystallites in the sulfided catalyst (5, 6). We investigated the effect of fluorination on the elementary reactions involved in the HDN of *o*-toluidine over unpromoted and nickel-promoted W/Al_2O_3 catalysts (8) and found that fluorine increased the activity of the hydrogenation of the aromatic ring and the breaking of the C(sp^2)–N bond. Complementary TPS, XPS, QEXAFS, and XANES investigations showed that fluorination affected the sulfidation process and the composition of the sulfided catalysts (9, 10).

Reliable methods for the determination of the dispersion of metal sulfides are not available yet. Consequently, it is very difficult to conclude that the difference in catalytic activity is due either to a better dispersion or to a difference in the catalytic sites. Kinetic studies might reveal a difference in the intrinsic properties of the active sites on different catalysts. In principle, kinetic studies determine two types of parameters, i.e., rate constants and equilibrium adsorption constants. Whereas the former parameters include the number of sites, the latter do not depend principally on the number of sites but rather on the quality of the sites. Therefore, investigating the effects of fluorination and promoter incorporation on the kinetic parameters is an alternative way for gaining a better understanding of the promotional effect of fluorine and of the promoter on the activities of HDS and HDN. The kinetic investigation of the effects of fluorine and nickel on the HDN of 2-methylcyclohexylamine showed that fluorine did not change the intrinsic properties of the active sites but decreased their number and that nickel slightly increased the adsorption of 2-methylcyclohexylamine on the active sites (11). The work presented here is a continuation of our earlier work, the aim of which was to gain a fundamental understanding of the role of fluorine and nickel in HDN catalysts.

Although it is well known that the addition of nickel or cobalt to molybdenum and of nickel to tungsten-hydrotreating catalysts strongly enhances their activity, several fundamental questions regarding the promotional effect of cobalt and nickel remain unanswered (12, 13). Several models have been proposed to explain the promotional effect of cobalt on molybdenum, the most widely accepted model being the so-called "CoMoS" phase model (14, 15).

[1] To whom correspondence should be addressed. Fax: 41-1-6321162. E-mail: prins@tech.chem.ethz.ch.

0021-9517/01 $35.00

Analogously, the promotional effect of nickel on molybdenum and tungsten catalysts is attributed to the formation of "NiMoS" and "NiWS" phases, respectively. However, why the nickel-promoted molybdenum or tungsten catalysts have higher activity is not yet clear. Theoretical calculations suggest that the promoters weaken the sulfur binding energy, decrease the equilibrium sulfur coverage, and hence increase the number of vacancies, which are the active sites (16, 17). Because the loss of hydrogenation activity of a Ni–Mo catalyst in the HDN of indoline was related to a measured decrease in the nickel content on the catalyst surface, Zhang *et al.* suggested that sulfur vacancies associated with nickel in the NiMoS phase are responsible for most of the hydrogenation activity (18).

Classically prepared tungsten catalysts are only partially sulfided and are a mixture of W(VI) oxysulfides and WS_2 (9, 10, 19–21). To interpret the kinetic data more precisely, we used catalysts prepared from ammonium tetrathiotungstate, which can be fully sulfided (9, 10), to study the kinetics of the HDN of *o*-toluidine. Preliminary results of investigations of the effect of fluorine on the kinetics of the HDN of *o*-toluidine on the unpromoted tungsten catalysts have been reported elsewhere (22). We extended the study of tungsten catalysts to include nickel-promoted tungsten catalysts.

EXPERIMENTAL

The catalysts used in this study were prepared from ammonium tetrathiotungstate (ATT). The preparation and the characterization results of the catalysts ATT/Al_2O_3, ATT/Al_2O_3–F, Ni–ATT/Al_2O_3, and Ni–ATT/Al_2O_3–F were presented elswhere (9, 10). All the catalysts contained 10 wt% of tungsten; the nickel-promoted catalysts contained 1 wt% of nickel, and the fluorine content of the fluorinated catalysts was 1 wt%. Prior to the reaction, the catalysts were treated *in situ* with a mixture of H_2S (10 mol%) and H_2 (90 mol%) at 400°C and 1.5 MPa for 4 h. Then, the temperature was lowered to 370°C, the pressure was increased to 3.0 MPa, and the liquid feed was introduced to the reactor by means of a high-pressure pump. The reactants were *o*-toluidine (TOL) and cyclohexene (CHE) with *n*-octane as the solvent and *n*-heptane as the internal standard. Dimethyl disulfide was added to the feed to generate H_2S (6 kPa) in the reaction stream. The partial pressure of TOL varied from 1 to 9 kPa, while the partial pressures of CHE, *n*-octane, and *n*-heptane were kept constant at 9, 75, and 5 kPa, respectively. The partial pressure of H_2 was varied slightly from 2900 to 2920 kPa so that the total pressure remained constant at 3.0 MPa. The amount of the catalyst varied from 0.1 to 1.2 g to obtain different levels of conversion of TOL and CHE. We checked that the conversion of TOL on a catalyst was the same at the same weight time when using different amounts of catalyst. Reaction products were analyzed with an on-line gas chromatograph equipped with a 50-m CP Sil-5 fused silica capillary column and a flame ionization detector. Samples were taken after 20 h on stream when the activity of the catalyst was stable. At the end of the experiments, the initial reaction conditions were repeated and the activities of the catalysts were found to differ by less than 5%.

RESULTS

HDN of o-Toluidine

The HDN of TOL proceeds via two pathways: the direct C(sp^2)–N bond breaking to toluene (T) and the hydrogenation of the phenyl ring followed by C(sp^3)–N bond breaking of 2-methylcyclohexylamine (MCHA) to methylcyclohexane (MCH) and methylcyclohexene (MCHE) (Fig. 1) (8, 23). Under the present reaction conditions, the hydrogenation intermediate MCHA was not detected in the HDN products of TOL on any of the catalysts, because the hydrogenation of TOL to MCHA is slow relative to the subsequent reactions of MCHA to MCHE and MCH. The products, MCHE and MCH, will be referred to as 'the hydrogenation products,' because they are formed via path 2. It was claimed that C(sp^2)–N bond breaking and the hydrogenation of the phenyl ring occur on different catalytic sites (18, 24–27); therefore, if this is true, then different equilibrium adsorption constants of TOL should, in principle, be considered for these two active sites. The yield of the hydrogenation products increased linearly with the conversion of TOL for all catalysts, as shown for the Ni–ATT/Al_2O_3 catalyst in Fig. 2. Therefore, the selectivities of the hydrogenation products and of toluene do not depend on the initial partial pressure of TOL. This means that it is possible to use the same adsorption constant of TOL for both reaction paths. The adsorption of the nitrogen-free hydrocarbon products and ammonia is much weaker than that of a nitrogen-containing reactant (23, 28) and can be ignored in the Langmuir–Hinshelwood rate equation for

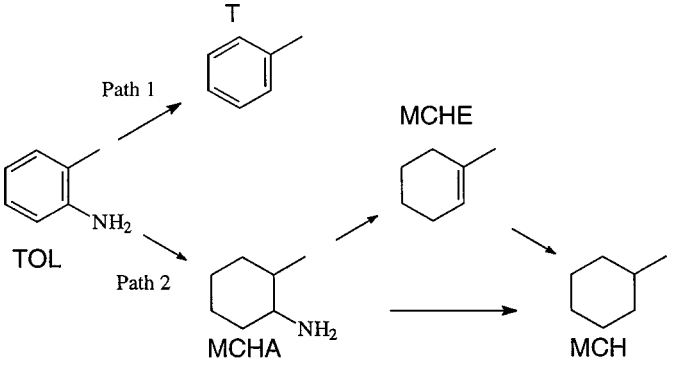

FIG. 1. HDN network of *o*-toluidine.

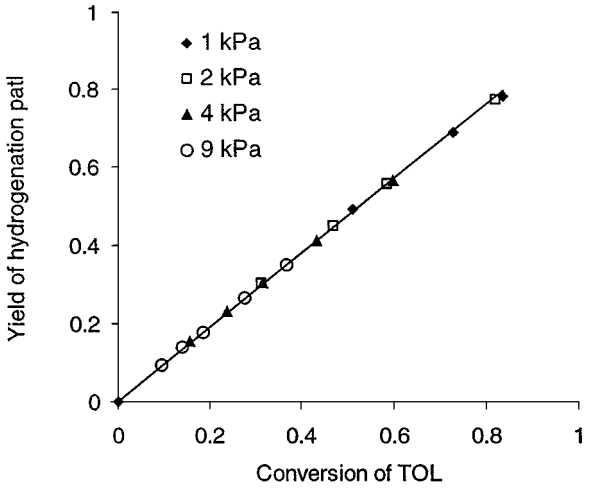

FIG. 2. Yield of the products of the hydrogenation path versus conversion of *o*-toluidine at 345°C and 3.0 MPa on Ni–ATT/Al_2O_3 at different partial pressures of *o*-toluidine.

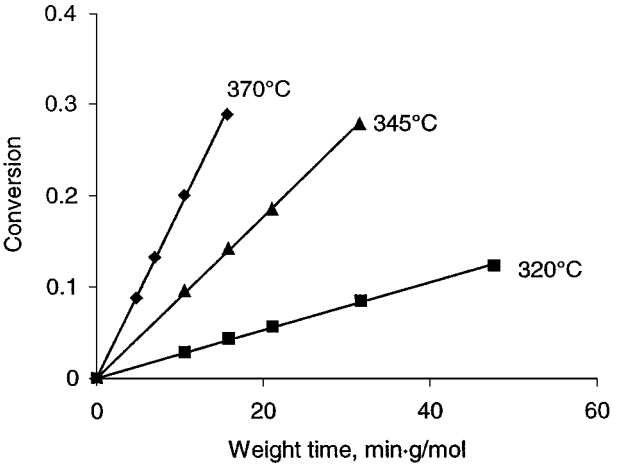

FIG. 3. Conversion versus weight time in the HDN of 9 kPa *o*-toluidine on Ni–ATT/Al_2O_3 at 3.0 MPa.

the HDN of TOL,

$$\frac{dP_{TOL}}{d\tau} = -\frac{(k_1 + k_2)K_{TOL}P_{TOL}}{1 + K_{TOL}P_{TOL}}, \qquad [1]$$

where P_{TOL} is the partial pressure of TOL, τ the weigh time, k_1 the rate constant for path 1, k_2 the rate constant for path 2, and K_{TOL} the equilibrium adsorption constant of TOL.

Direct simulation of the partial pressure of the reactants versus weight time, using Eq. [1], did not give unique parameter values, as has been addressed before (11, 29, 30). To obtain unique parameters, one of the parameters must be determined independently, as for the HDN of MCHA (11). At a high partial pressure of TOL, $K_{TOL}P_{TOL} \gg 1$, and Eq. [1] simplifies to the zero-order equation,

$$X_{TOL} = \frac{k_1 + k_2}{P^0_{TOL}} \cdot \tau, \qquad [2]$$

where X_{TOL} is the conversion and P^0_{TOL} the initial partial pressure of TOL. The plots are linear up to a TOL conversion of 30%. As an example, Fig. 3 gives the conversion of TOL over the Ni–ATT/Al_2O_3 catalyst versus weight time when the initial partial pressure of TOL is 9 kPa. In this way, the sums of the rate constants for the overall conversion of TOL, $k_1 + k_2$, were obtained for all the catalysts. Once $k_1 + k_2$ was determined, the adsorption constant K_{TOL} could be determined uniquely by varying the initial partial pressure of TOL (1, 2, 4, and 9 kPa) and by doing a nonlinear regression analysis of the experimental data using MacroMath Scientist 2.0 software, according to Eq. [1]. The results are given in Table 1. The statistical evaluation of the goodness-of-fit gave the standard deviations of the parameters, which are presented in parentheses in Table 1. Under the present conditions, paths 1 and 2 in the HDN of TOL are parallel reactions (8, 23); the selectivity of the C(sp^2)–N bond breaking is equal to $k_1/(k_1 + k_2)$ and that of the hydrogenation is equal to $k_2/(k_1 + k_2)$. Thus, from the overall rate constants $k_1 + k_2$ and the selectivity of the products, the individual values of k_1 and k_2 were obtained (Table 1).

Figure 4 shows the temperature dependence of the rate constants of paths 1 and 2 and of the equilibrium adsorption constant of TOL on the Ni–ATT/Al_2O_3 catalyst. The activation energies are given in Table 2, with the standard deviations in parentheses. The equilibrium adsorption constant of TOL on the unpromoted tungsten catalysts hardly changed with temperature. Therefore, the heat of adsorption of TOL on the unpromoted catalysts is too low to be determined accurately. The heat of adsorption of TOL on the nickel-promoted catalysts and its standard deviation are given in Table 2.

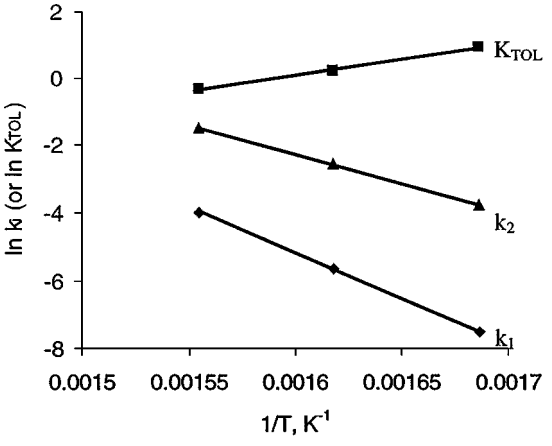

FIG. 4. Temperature dependence of the rate constants of paths 1 (k_1) and 2 (k_2) and the equilibrium adsorption constant of *o*-toluidine (K_{TOL}) for the HDN of *o*-toluidine on Ni–ATT/Al_2O_3 at 3.0 MPa.

TABLE 1

Kinetic Parameters for the HDN of *o*-Toluidine at 3.0 MPa (k_1 and k_2 in kPa mol min^{-1} g^{-1} and K_{TOL} in kPa^{-1})

		ATT/Al_2O_3	ATT/Al_2O_3–F	Ni–ATT/Al_2O_3	Ni–ATT/Al_2O_3–F
370°C	$k_2/(k_1+k_2)$	0.93	0.93	0.92	0.91
	k_1	0.002	0.003	0.02	0.02
	k_2	0.022	0.033	0.22	0.26
	K_{TOL}	1.1 (0.2)	1.3 (0.2)	0.72 (0.1)	0.87 (0.1)
345°C	$k_2/(k_1+k_2)$	0.93	0.94	0.96	0.95
	k_1	0.001	0.001	0.004	0.004
	k_2	0.009	0.013	0.076	0.078
	K_{TOL}	1.1 (0.3)	1.4 (0.3)	1.2 (0.3)	1.4 (1.2)
320°C	$k_2/(k_1+k_2)$	0.93	0.94	0.98	0.97
	k_1	0.0003	0.0003	0.001	0.001
	k_2	0.0037	0.0054	0.023	0.024
	K_{TOL}	1.2 (0.3)	1.4 (0.3)	2.5 (0.5)	2.4 (0.3)

Hydrogenation of Cyclohexene

The elementary reactions involved in the HDN of MCHA were studied separately, using MCHA as the model compound (11). Another elementary reaction in the HDN network of TOL is the hydrogenation of MCHE to MCH. The hydrogenation of an alkene requires different active sites than the hydrogenation of a phenyl ring on sulfide catalysts (8, 27). Therefore, different adsorption constants of TOL must be used in kinetic calculations of the HDN of TOL and the hydrogenation of CHE in the presence of TOL. The rate equation for the hydrogenation of CHE in the presence of TOL can be expressed as

$$\frac{dP_{CHE}}{d\tau} = -\frac{k_{CHE}K_{CHE}P_{CHE}}{1+K_{TOL}^{CHE}P_{TOL}+K_{CHE}P_{CHE}}, \qquad [3]$$

where P_{CHE} is the partial pressure of CHE, τ is the weight time, k_{CHE} and K_{CHE} are the rate and equilibrium adsorption constants of CHE respectively, K_{TOL}^{CHE} is the equilibrium adsorption constant of TOL on the CHE reaction sites, and P_{TOL} is the partial pressure of TOL. Since $K_{CHE} \sim 0.01\ kPa^{-1}$ (23) and $P_{CHE} = 9$ kPa, the term $K_{CHE}P_{CHE}$ was ignored.

Figure 5 shows that the conversion of CHE decreases with increasing partial pressure of TOL, showing that TOL inhibits the hydrogenation of CHE. In the simultaneous reactions of CHE and TOL, the decrease in the partial pressure of TOL (Eq. [3]) is very small at low conversion of TOL. The hydrogenation of CHE in the presence of TOL was, therefore, reduced to a pseudo-first-order reaction by making the partial pressure of TOL in the denominator of Eq. [2] equal to the initial value. Thus, Eq. [3] was simplified to

$$\ln(1-X_{CHE}) = k'_{CHE}\tau, \qquad [4]$$

where

$$k'_{CHE} = \frac{k_{CHE}K_{CHE}}{1+K_{TOL}^{CHE}P_{TOL}^{0}}. \qquad [5]$$

From the slopes of the plots of $\ln(1-X_{CHE})$ against weight time, the apparent rate constants for the hydrogenation of CHE at different initial partial pressures of TOL were obtained. The reciprocal of the apparent rate constant for the hydrogenation of CHE is proportional to the initial partial pressures of TOL. Thus, values for K_{TOL}^{CHE} and $k_{CHE}K_{CHE}$ were estimated from the slopes and intercepts of the plots of $1/k'_{CHE}$ against the initial partial pressure of TOL at different temperatures (cf. Fig. 6 for Ni–ATT/Al_2O_3). Using these values as starting points for the CHE rate and adsorption constants and the rate and adsorption constants for the HDN of TOL as fixed parameters, unequivocal kinetic parameters for the hydrogenation of CHE in the presence

TABLE 2

Temperature Dependence of Rate Constants and Equilibrium Constants in the HDN of *o*-Toluidine at 3.0 MPa ($k_i = A_i \exp(-E_i/RT)$, $K_{TOL} = K_0 \exp(-\Delta H/RT)$)

	ATT/Al_2O_3	ATT/Al_2O_3–F	Ni–ATT/Al_2O_3	Ni–ATT/Al_2O_3–F
E_1 (kJ/mol)	114 (7)	133 (15)	224 (19)	216 (10)
A_1 (kPa mol min^{-1} g^{-1})	3E + 6	2E + 8	2E + 16	8E + 15
E_2 (kJ/mol)	114 (10)	116 (10)	142 (12)	151 (10)
A_2 (kPa mol min^{-1} g^{-1})	4E + 7	8E + 7	1E + 10	5E + 11
$-\Delta H$ (kJ/mol)	—	—	79 (10)	63 (10)
K_0 (kPa^{-1})	—	—	1E − 6	1E − 5

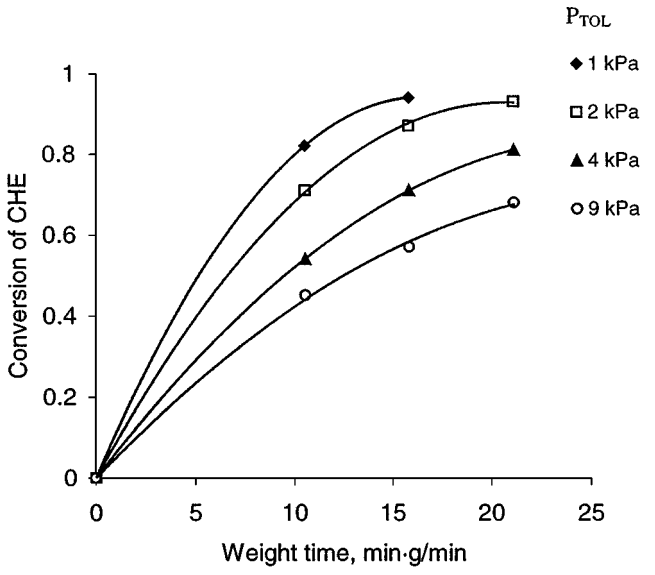

FIG. 5. Conversion of cyclohexene versus weight time in the presence of different partial pressures of *o*-toluidine at 345°C and 3.0 MPa on Ni–ATT/Al_2O_3.

of TOL were obtained through simulation of the experimental data with Eqs. [1] and [3] (Table 3).

The rate and adsorption constants of CHE cannot be separated under the present conditions. Thus, we obtained only the sum of the activation energy and the heat of adsorption of CHE from the temperature dependence of $k_{CHE}K_{CHE}$ (Table 3). The adsorption constant of TOL on the CHE reaction site is too small to reliably determine the heat of adsorption of TOL on the CHE reaction sites.

DISCUSSION

The hydrogenation of the phenyl ring is the major path in the HDN of TOL on the alumina-supported tungsten sulfide catalyst in the presence of H_2S, as already observed in the HDN of other substituted anilines on molybdenum- and tungsten-based sulfide catalysts (23, 24, 29, 31–34). The hydrogenation path contributes more than 90% to the overall conversion of TOL for the tungsten sulfide catalysts (Table 1). It is still unclear as to how the direct C(sp^2)–N bond breaking from TOL to toluene takes place. This reaction is often referred to as hydrogenolysis (24, 31, 33), but it is unlikely that the C–N bond breaks on sulfide catalysts in the same way as the C–C bond in hydrocarbon on metal catalysts. Many experimental results have shown that the mechanism of C(sp^2)–N bond breaking differs from C(sp^3)–N bond breaking (8, 24, 27, 32, 35–37), which occurs by Hofmann-type elimination or nucleophilic substitution (23, 24, 38–41). C(sp^2)–N bond breaking behaves like hydrogenation (8); it is enhanced by hydrogen and inhibited by H_2S (37, 38). Furthermore, it depends on the aromaticity of the phenyl ring of aniline-type compounds, while the cleavage of C(sp^3)–N bonds is determined by the basicity of the nitrogen atom (24). Therefore, a possible mechanism for the direct conversion of TOL to toluene might be the partial hydrogenation of TOL to dihydrotoluidine followed by elimination of ammonia as suggested by Girgis and Gates (42) (Fig. 7). A similar mechanism has also been proposed for the conversion of dibenzothiophene (43). Another explanation may be that the arylamine undergoes C–N bond homolysis on the surface of the metal sulfide, as proposed for the C–S bond scission in the homogeneous desulfurization of thiols on $Cp'_2Mo_2Co_2S_3(CO)_4$ clusters (44). In the latter reaction, the thiol binds to a "latent vacancy" by reorganization of the metal and sulfur atoms of the metal–sulfur cluster (Scheme 1). The strong bonding of the sulfur atom of the SR fragment to several metal atoms weakens the C–S bond. This leads to C–S bond breaking and RH formation. A similar HDN mechanism may occur by the bonding of a RNH fragment to the metal sulfide surface.

The selectivity of the hydrogenation products hardly changes with temperature over the unpromoted tungsten catalysts (Table 1). This is due to the very similar activation energies of paths 1 and 2 (within the uncertainties of the determination) over the unpromoted catalysts (Table 2). This result can be explained by the common intermediate mechanism, as indicated in Fig. 7. For the ATT/Al_2O_3 catalyst, the ratio of the rate constants for the elimination of ammonia from MCHA (11) and for the conversion of TOL (Table 1) is 49. Even if we assume that the rate of elimination of ammonia from dihydrotoluidine to form toluene is lower than the rate of elimination of ammonia from MCHA, the rate of elimination of ammonia from dihydrotoluidine might still be higher than the rate of the hydrogenation of TOL. In that case, the observed activation energy for the formation

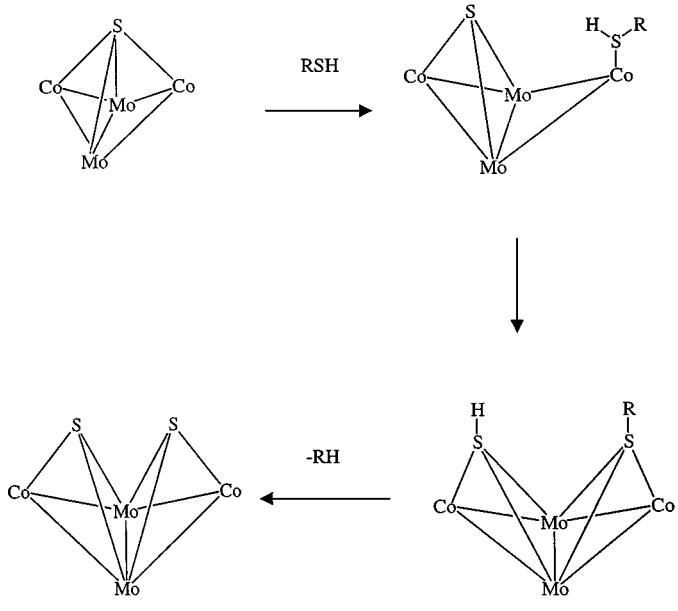

SCHEME 1

TABLE 3

Kinetic Parameters for the Hydrogenation of CHE at 3.0 MPa (k_{CHE} in kPa mol min^{-1} g^{-1}, K_{TOL}^{CHE} and K_{CHE} in kPa^{-1}, $k_{CHE}K_{CHE} = (k^{\circ}_{CHE}K^{\circ}_{CHE})\exp(-(E_{CHE} + \Delta H_{CHE})/RT)$)

		ATT/Al_2O_3	ATT/Al_2O_3–F	Ni–ATT/Al_2O_3	Ni–ATT/Al_2O_3–F
370°C	$k_{CHE}K_{CHE}$	0.014 (0.001)	0.022 (0.001)	0.33 (0.03)	0.36 (0.01)
	K_{TOL}^{CHE}	0.03 (0.01)	0.03 (0.01)	0.24 (0.06)	0.32 (0.02)
345°C	$k_{CHE}K_{CHE}$	0.0075 (0.0001)	0.011 (0.001)	0.18 (0.01)	0.20 (0.01)
	K_{TOL}^{CHE}	0.04 (0.01)	0.05 (0.01)	0.32 (0.04)	0.37 (0.03)
320°C	$k_{CHE}K_{CHE}$	0.0045 (0.0004)	0.0065 (0.0001)	0.088 (0.003)	0.089 (0.003)
	K_{TOL}^{CHE}	0.06 (0.01)	0.08 (0.01)	0.37 (0.02)	0.41 (0.02)
	$E_{CHE} + \Delta H_{CHE}$ (kJ/mol)	72 (10)	78 (10)	84 (10)	89 (10)

of toluene would be equal to the activation energy of the hydrogenation of TOL over the ATT/Al_2O_3 catalyst.

On the nickel-promoted catalysts, the selectivity of the hydrogenation products decreases with increasing reaction temperature (Table 1), which is explained by the higher activation energy for path 1 than for path 2 over the nickel-promoted catalysts (Table 2). The ratio of the rate constants for the elimination of ammonia from MCHA (11) and for the conversion of TOL (Table 1) is only 6 for the Ni–ATT/Al_2O_3 catalyst. This is due to the much higher hydrogenation rate of the Ni–ATT/Al_2O_3 catalyst than that of the ATT/Al_2O_3 catalyst at about the same elimination rate. Thus, the rate of elimination of ammonia from dihydrotoluidine might not be higher than the rate of hydrogenation of TOL for the Ni–ATT/Al_2O_3 catalyst. In that case, the activation energy for the formation of toluene is not the same as that for the hydrogenation of TOL. This may explain why paths 1 and 2 show different activation energies over the Ni–ATT/Al_2O_3 catalyst and the same activation energy over the ATT/Al_2O_3 catalyst.

It is widely accepted that there are two main types of active sites on molybdenum and tungsten sulfide catalysts. Type I consists of sulfur vacancies associated with metal atoms, and type II consists of surface SH groups or sulfur anions (14, 15, 18, 33, 35, 45–49). The fact that H_2S inhibits C(sp^2)–N bond breaking (37, 38) suggests that sulfur vacancies are necessary for this reaction to occur. In general, there are two kinds of sulfur vacancies on the nickel-promoted catalysts, one associated with molybdenum (or tungsten) atoms and the other with nickel in the Ni–Mo–S (or Ni–W–S) phase (18, 46, 49–52). It has been proposed that vacancies involving nickel are mainly responsible for the hydrogenation (18, 49, 53, 54). Consistent with this proposal, we found that the incorporation of nickel in the tungsten catalysts hardly affected the HDN of MCHA (8, 11) but significantly increased the HDN of TOL (Table 1).

Nickel increases both the activation energy and the heat of adsorption of TOL (Table 1). This means that the nickel-associated vacancies are different in nature than the tungsten-associated vacancies. The equilibrium adsorption constant of TOL hardly changes with temperature on the unpromoted tungsten catalysts, while a clear increase in the equilibrium adsorption constant of TOL on

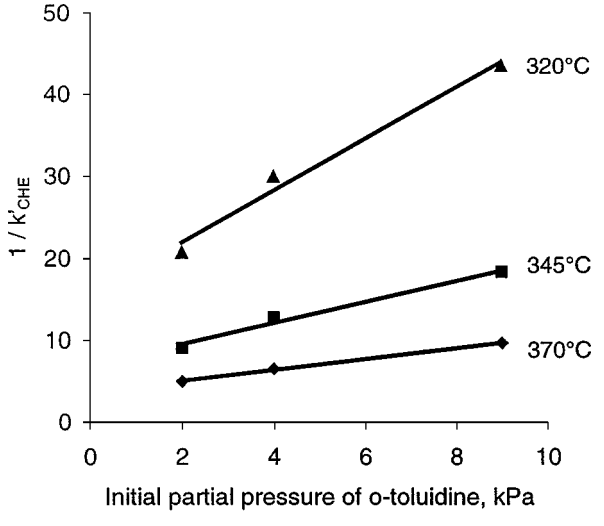

FIG. 6. $1/k_{CHE}$ versus initial partial pressure of *o*-toluidine in the hydrogenation of cyclohexene in the presence of *o*-toluidine on Ni–ATT/Al_2O_3 at 3.0 MPa.

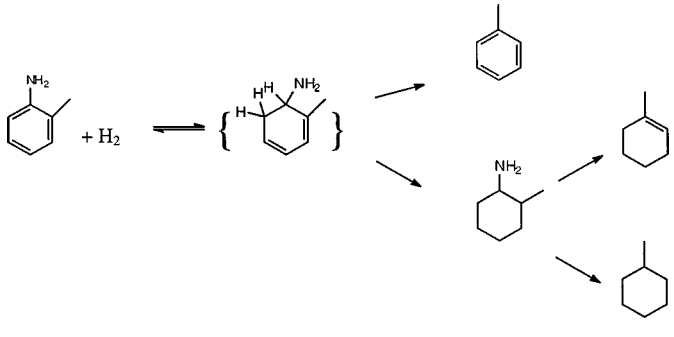

FIG. 7. Reaction scheme for the HDN of *o*-toluidine via a dihydrotoluidine intermediate.

the nickel-promoted catalysts is observed with decreasing temperature (Table 1). The reason for this behavior is not clear. We made several checks to eliminate the possibilities of experimental inconsistencies. It may be that the degree of sulfidation of the catalyst surface is more sensitive to temperature for the unpromoted catalysts than for the Ni-promoted catalysts. Although the H_2S/H_2 ratio was kept constant at 0.002 in all the experiments at all temperatures, this does not mean that the relative amount of sulfur (and thus of the vacancies) is the same at all temperatures. Even at the same H_2S/H_2 ratio, more sulfur vacancies are to be expected at higher temperature because of the entropy effect on the $^*S + H_2 \rightleftharpoons H_2S + ^*$ equilibrium, where $^*S$ denotes the "adsorbed" sulfur atom and * is a sulfur vacancy. The equilibrium constant K_{TOL} would then be considered to consist of the product of the real adsorption constant K'_{TOL} and the constant K^* of this surface sulfur equilibrium, $K_{TOL} = K'_{TOL} \cdot K_*$. The constant K'_{TOL} decreases with increasing temperature, but K^* increases, and thus the number of sulfur vacancies also increases. Theoretical calculations showed that the sulfur binding energy is higher for unpromoted sulfided molybdenum structures than for the Co–Mo–S and Ni–Mo–S structures (16, 17). Analogously, if the sulfur atoms are more strongly bonded to unpromoted-tungsten structures than to nickel-promoted structures, the temperature dependence of this sulfur equilibrium is stronger for the ATT catalysts than for the Ni–ATT catalysts. Consequently, the temperature dependency of the ATT catalysts is less than that of the Ni–ATT catalysts.

The equilibrium adsorption constant of TOL on the CHE hydrogenation site is much smaller than that on its own hydrogenation site (cf. Tables 1 and 3), just as the equilibrium adsorption constants of quinoline and *o*-propylaniline on the alkene hydrogenation site are much smaller than those on the site of the phenyl ring hydrogenation on $Ni–Mo/Al_2O_3$ catalysts (27). These results prove that the hydrogenation of the phenyl ring occurs on a different site than the hydrogenation of an alkene. Because the π-electron moiety interacts with the active centers in the reaction of aniline-type compounds on sulfide catalysts by flat adsorption (24), there must be more vacancies to accommodate and activate the aromatic ring in the reaction of TOL, while for the hydrogenation of an alkene one vacancy may be sufficient. In the C(sp^3)–N bond breaking of MCHA, however, the basicity of the amine moiety determines the reactivity (24) because the adsorption of MCHA on the active sites occurs via its amine moiety, which is strongly basic.

In the presence of MCHA, the hydrogenation of CHE is strongly inhibited (8), while in the presence of TOL, the conversion of CHE is still substantial (Fig. 5). Thus, the inhibitory effect of MCHA on alkene hydrogenation is much stronger than that of TOL; for instance, at 370°C, $K_{TOL}^{CHE} = 0.24\ kPa^{-1}$ and $K_{MCHA}^{CHE} > 2.5\ kPa^{-1}$ (estimated from the results of the simultaneous reactions of CHE and MCHA). This is in line with the stronger basicity of MCHA ($pK_a = 10$) than that of TOL ($pK_a = 4.4$) (57, 58). Therefore, it is probable that both TOL and MCHA adsorb on the alkene hydrogenation site via their amine groups. TOL adsorbs on its own hydrogenation site via the aromatic moiety while it adsorbs on the alkene hydrogenation site via its amine group; this explains why the equilibrium adsorption constants of TOL are so different on the two sites. The much larger equilibrium adsorption constants of TOL on the CHE reaction site on the nickel-promoted catalysts than on the unpromoted catalysts (Table 3) confirm that there is a fundamental difference between the nickel-associated vacancy and the tungsten-associated vacancy.

Many explanations have been given in the literature for the effect of fluorine on hydrotreating catalysts (2, 3, 5–7). The enhanced acidity of fluorinated catalysts has been considered to be one of the main factors that accounts for the promotional effect of fluorine on HDS and HDN (2, 5–7, 59) since it was observed that fluorine enhanced the acid-catalyzed isomerization and cracking reactions (2, 7, 59, 60). Indeed, C(sp^3)–N bond breaking requires acidic sites as well, be it elimination or nucleophilic substitution. However, we found that fluorine hardly influenced the elimination but that it decreased the nucleophilic substitution in the HDN of MCHA (11). The acid sites related to fluorine on alumina are responsible for isomerization and cracking (7, 61, 62), but they are not available for isomerization of CHE when a basic nitrogen-containing compound is present in the feed. As we showed before (8), in that case, the acidic sites are completely inhibited by the basic molecules, and increased acidity cannot explain the role of fluorine in HDN.

Within the uncertainty of the measurement, fluorine changes neither the activation energies nor the heat of adsorption of toluidine (Table 2) in the ATT/Al_2O_3 and the $Ni–ATT/Al_2O_3$ catalysts. This proves that, in both cases, fluorine does not change the nature of the active sites. The promotional effect of fluorine on the HDN of TOL, therefore, does not result from a change in the intrinsic activity of the sites but from an increase in the number of active sites. For classic alumina-supported tungsten catalysts, which can only be partially sulfided at 400°C, fluorine was considered to improve the sulfidation (5, 6) and, thus, the number of active sites for HDN. However, TPS measurements (9, 10) and sulfur analysis (6) showed that fluorine only slightly increased the degree of sulfidation of tungsten, while XPS results showed that the fluorinated catalysts had a lower W(IV)/W(VI) ratio than their fluorine-free counterparts after sulfidation (6, 9, 10). Furthermore, in the present study we used fully sulfided catalysts; therefore, the extent of sulfidation cannot be a key factor in the effect of fluorination.

Our results unequivocally show that the character of the catalytic sites is not influenced by fluorine. This was to

be expected because it is well known that fluorine is located on the alumina support and not on the active metal sulfide. This means that the fluorine effect must be indirect. How does fluorination of the alumina support influence the number of sites of the metal sulfide phase? A higher dispersion of the metal sulfide cannot be the explanation because fluorination decreases the dispersion of the tungsten phase on the catalyst surface (6, 11, 63). Transmission electron microscopy measurements showed that fluorination increased the stacking and the length of WS_2 slabs (5, 64). Our QEXAFS results also showed that fluorine increased the size of the WS_2 crystallites (9). WS_2 crystallites are well dispersed on fluorine-free catalysts but aggregate to bigger particles on the fluorinated catalysts. As discussed above, the hydrogenation of alkenes requires one vacancy, the adsorption of MCHA is through its amine group, and the hydrogenation of TOL requires more vacancies to accommodate the phenyl ring. The bigger WS_2 particles may contain more adjacent vacancies, which are the active centers for TOL hydrogenation. Furthermore, the higher stacking provides more space for the flat adsorption of TOL on these active centers. Considering that fluorine hardly influences the hydrogenation of CHE and the HDN of MCHA and that it increases the hydrogenation of TOL, we conclude that the higher stacking of WS_2 is the origin of the promotional effect of fluorine on the HDN of TOL.

CONCLUSIONS

The fact that the two pathways in the HDN of TOL, one leading to toluene and the other to MCHE and MCH, show similar activation energies on unpromoted tungsten catalysts suggests the existence of a common intermediate, dihydrotoluidine, for the formation of toluene and MCHA. The fact that the selectivities of toluene and MCHE plus MCH do not depend on the partial pressure of TOL also suggests that these two pathways go through the same intermediate.

The equilibrium adsorption constants of TOL on the TOL hydrogenation site and on the CHE hydrogenation site are very different, demonstrating that the site for the hydrogenation of a phenyl ring differs from that for the hydrogenation of an alkene. The former site probably consists of more vacancies that accommodate TOL via its π-electrons; the latter site has one vacancy only, upon which TOL adsorbs via the amine group.

Fluorination does not cause significant changes in the activation energy and the heat of adsorption of TOL on the sites for the hydrogenation of TOL and CHE. This indicates that the promotional effect of fluorine is not due to a change in the intrinsic properties of the active sites but to an increase in the number of sites. Fluorine apparently affects the activity of the catalyst by modifying the morphology of the active phases. The larger WS_2 particles have more adjacent vacancies where TOL can adsorb and react, and the higher stacking favors the adsorption of TOL on the catalyst via the phenyl π-system. The hydrogenation of CHE does not require adjacent vacancies, and therefore, the change in the morphology of the catalyst surface has little effect on it. Incorporation of nickel in the tungsten catalysts creates a new type of active site, a nickel-associated sulfur vacancy with a much higher activity for hydrogenation than the tungsten-associated sulfur vacancy.

REFERENCES

1. Muralidhar, G., Massoth, F. E., and Shabtai, J., *J. Catal.* **85**, 44 (1984).
2. Jiratova, K., and Kraus, M., *Appl. Catal. A* **27**, 21 (1986).
3. Papadopoulou, Ch., Lycourghiotis, A., Grange, P., and Delmon, B., *Appl. Catal. A* **38**, 255 (1988).
4. Kwak, C., Lee, J. J., Bae, J. S., Choi, K., and Moon, S. H., *Appl. Catal. A* **200**, 233 (2000).
5. Benitez, A., Ramirez, J., Vazquez, A., Acosta, D., and Lopez Agudo, A., *Appl. Catal. A* **133**, 103 (1995).
6. Benitez, A., Ramirez, J., Fierro, J. L. G., Lopez Agudo, A., *Appl. Catal. A* **144**, 343 (1996).
7. Boorman, P. M., Kydd, R. A., Sarbak, Z., and Somogyvari, A., *J. Catal.* **106**, 544 (1987).
8. Sun, M., Bussell, M. E., and Prins, R., *Appl. Catal. A* **216**, 103 (2001).
9. Sun, M., Burgi, Th., Cattaneo, R., and Prins, R., *J. Catal.* **197**, 172 (2001).
10. Sun, M., Burgi, Th., Cattaneo, R., van Langeveld, A. D., and Prins, R., submitted for publication.
11. Sun, M., and Prins, R., *J. Catal.* **201**, 138 (2001).
12. Topsøe, H., Clausen, B. S., and Massoth, F. E., "Hydrotreating Catalysis." Springer Verlag, Berlin, 1996.
13. Prins, R., de Beer, V. H. J., and Somorjai, G. A., *Catal. Rev.-Sci. Eng.* **31**, 1 (1989).
14. Topsøe, H., Clausen, B. S., Candia, R., Wivel, C., and Mørup, S., *J. Catal.* **68**, 433 (1981).
15. Wivel, C., Candia, R., Clausen, B. S., Mørup, S., and Topsøe, H, *J. Catal.* **68**, 453 (1981).
16. Byskov, L. S., Nørskov, J. K., Clausen, B. S., and Topsøe, H., *J. Catal.* **187**, 109 (1999).
17. Raybaud, P., Hafner, J., Kresse, G., Kasztelan, S., and Toulhoat, H., *J. Catal.* **190**, 128 (2000).
18. Zhang, L., Karakas, G., and Ozkan, U. S., *J. Catal.* **178**, 457 (1998).
19. Ng, K. T., and Hercules, D. M., *J. Phys. Chem.* **80**, 2094 (1976).
20. Breysse, M., Cattenot, M., Decamp, T., Frety, R., Gachet, C., Lacroix, M., Leclerq, C., de Mourgues, L., Portefaix, J. L., Vrinat, M., Houari, M., Grimblot, J., Kasztelan, S., Bonnelle, J. P., Housni, S., Bachelier, J., and Duchet, J. C., *Catal. Today* **4**, 39 (1988).
21. Scheffer, B., Mangnus, P. J., and Moulijn, J. A., *J. Catal.* **121**, 18 (1990).
22. Sun, M., and Prins, R., *Stud. Surf. Sci. Catal.* **133**, 581 (2001).
23. Rota, F., and Prins, R., *Top. Catal.* **11/12**, 327 (2000).
24. Moreau, C., Aubert, C., Durand, R., Zmimita, N., and Geneste, P., *Catal. Today* **4**, 117 (1988).
25. Okamoto, Y., Maezawa, A., and Imanaka, A., *J. Catal.* **120**, 29 (1989).
26. Massoth, F. E., Balusami, K., and Shabtai, J., *J. Catal.* **122**, 256 (1990).
27. Jian, M., and Prins, R., *Catal. Lett.* **50**, 9 (1998).
28. Satterfield, C. N., and Yang, S. H., *Ind. Eng. Chem. Proc. Des. Dev.* **23**, 11 (1984).
29. Jian, M., Kapteijn, F., and Prins, R., *J. Catal.* **168**, 491 (1997).
30. Jian, M., and Prins, R., *Ind. Eng. Chem. Res.* **37**, 834 (1998).
31. Olivé, J. L., Biyoko, S., Moulinas, C., and Geneste, P., *Appl. Catal. A* **19**, 165 (1985).

32. Schulz, H., Schon, M., and Rahman, N. M., *Stud. Surf. Sci. Catal.* **27**, 201 (1986).
33. Ho, T. C., *Catal. Rev.-Sci. Eng.* **30**, 117 (1988).
34. Durand, R., Geneste, P., Moreau, C., and Zmimita, N., *J. Catal.* **112**, 411 (1988).
35. Yang, S. H., and Satterfield, C. N., *J. Catal.* **81**, 168 (1983).
36. Shanthi, K., Pillai, C. N., and Kuriacose, J. C., *Appl. Catal. A* **46**, 241 (1989).
37. Rota, F., and Prins, R., *J. Mol. Catal. A: Chem.* **162**, 367 (2000).
38. Nelson, N., and Levy, R. B., *J. Catal.* **58**, 485 (1979).
39. Laine, R. M., *Catal. Rev.-Sci. Eng.* **35**, 459 (1983).
40. Perot, G., *Catal. Today* **10**, 447 (1991).
41. Cattenot, M., Portefaix, J. L., Afonso, J., Breysse, M., Lacroix, M., and Perot, G., *J. Catal.* **173**, 366 (1998).
42. Girgis, M. J., and Gates, B. C., *Ind. Eng. Chem. Res.* **30**, 2021 (1991).
43. Meille, V., Schulz, E., Lemaire, M., and Vrinat, M., *J. Catal.* **170**, 29 (1997).
44. Curtis, M. D., and Druker, S. H., *J. Am. Chem. Soc.* **119**, 1027 (1997).
45. Mcllvried, H. G., *Ind. Eng. Chem. Proc. Des. Dev.* **10**, 125 (1971).
46. Topsøe, N. Y., and Topsøe, H., *J. Catal.* **84**, 386 (1983).
47. Yang, S. H., and Satterfield, C. N., *Ind. Eng. Chem. Proc. Des. Dev.* **23**, 20 (1984).
48. Hadjiloizou, G. C., Butt, J. B., and Dranoff, J. S., *Ind. Eng. Chem. Res.* **31**, 2503 (1992).
49. Ozkan, U. S., Zhang, L., Ni, S., and Moctezuma, E., *J. Catal.* **148**, 181 (1994).
50. Satterfield, C. N., Modell, M., and Wilkens, J. A., *Ind. Eng. Chem. Proc. Des. Dev.* **19**, 154 (1980).
51. Topsøe, H., and Clausen, B. S., *Catal. Rev.-Sci. Eng.* **26**, 395 (1984).
52. Louwers, S. P. A., and Prins, R., *J. Catal.* **139**, 525 (1993).
53. Perot, G., Brunet, S., and Hamze, N., *in* "Proceedings, 9th International Congress on Catalysis, Calgary, 1988" (M. J. Phillips and M. Ternan, Eds.), Vol. 1, p. 19. Chem. Institute of Canada, Ottawa, 1988.
54. Ozkan, U. S., Ni, S., Zhang, L., and Moctezuma, E., *Energy Fuels* **8**, 249 (1994).
55. Pecoraro, T. A., and Chianelli, R. R., *J. Catal.* **67**, 430 (1981).
56. Nørskov, J. K., Clausen, B. S., and Topsøe, H., *Catal. Lett.* **13**, 1 (1992).
57. Smith, J. W., *in* "The Chemistry of the Amino Group" (S. Patai, Ed.), p. 161. Wiley Interscience, New York, 1968.
58. Yang, M. H., Grange, P., and Delmon, B., *Appl. Catal. A* **154**, L7 (1997).
59. Boorman, P. M., Kriz, J. F., Brown, J. R., and Ternan, M., *in* "Proc. 4th Int. Climax Conf. on Chemistry and Uses of Molybdenum" (H. F. Barry and P. C. H. Mitchell, Eds.), p. 192. Climax Comp., Ann Arbor, 1982.
60. Benitez, A., Ramirez, J., Cruz-Reyes, A., and Lopez Agudo, A., *J. Catal.* **172**, 137 (1997).
61. Boorman, P. M., Kydd, R. A., Sarbak, Z., and Somogyvari, A., *J. Catal.* **96**, 115 (1985).
62. Boorman, P. M., Kydd, R. A., Sarbak, Z., and Somogyvari, A., *J. Catal.* **100**, 287 (1986).
63. Ramirez, J., Cuevas, R., Lopez Agudo, A., Mendioroz, S., and Fierro, J. L. G., *Appl. Catal.* **57**, 223 (1990).
64. Ramirez, J., Castillo, P., Benitez, A., Vazquez, A., Acosta, D., and Lopez Agudo, A., *Appl. Catal.* **57**, 223 (1990).